Photosynthesis Research (2019) 142:137–151
https://doi.org/10.1007/s11120-019-00662-5

ORIGINAL ARTICLE

Red-shifted light-harvesting system of freshwater eukaryotic alga *Trachydiscus minutus* (Eustigmatophyta, Stramenopila)

Radek Litvín[1,2] · David Bína[1,2] · Miroslava Herbstová[1,2] · Marek Pazderník[1,3] · Eva Kotabová[1,3] · Zdenko Gardian[1,2] · Martin Trtílek[4] · Ondřej Prášil[1,3] · František Vácha[1,2]

Received: 29 May 2019 / Accepted: 22 July 2019 / Published online: 2 August 2019
© Springer Nature B.V. 2019

Abstract

Survival of phototrophic organisms depends on their ability to collect and convert enough light energy to support their metabolism. Phototrophs can extend their absorption cross section by using diverse pigments and by tuning the properties of these pigments via pigment–pigment and pigment–protein interaction. It is well known that some cyanobacteria can grow in heavily shaded habitats by utilizing far-red light harvested with far-red-absorbing chlorophylls *d* and *f*. We describe a red-shifted light-harvesting system based on chlorophyll *a* from a freshwater eustigmatophyte alga *Trachydiscus minutus* (Eustigmatophyceae, *Goniochloridales*). A comprehensive characterization of the photosynthetic apparatus of *T. minutus* is presented. We show that thylakoid membranes of *T. minutus* contain light-harvesting complexes of several sizes differing in the relative amount of far-red chlorophyll *a* forms absorbing around 700 nm. The pigment arrangement of the major red-shifted light-harvesting complex is similar to that of the red-shifted antenna of a marine alveolate alga *Chromera velia*. Evolutionary aspects of the algal far-red light-harvesting complexes are discussed. The presence of these antennas in eustigmatophyte algae opens up new ways to modify organisms of this promising group for effective use of far-red light in mass cultures.

Keywords Light-harvesting protein · Violaxanthin · Eustigmatophyta · Red-shifted LHC · Oligomeric LHC · Chromatic acclimation

Introduction

Photosystems are the key photosynthetic enzymes which convert light energy to electrochemical potentials. Due to the low energy density of natural light, the photosystems use light-harvesting antennas to extend their absorption cross-sections. The light-harvesting antennas are pigment–protein complexes in which the protein serves as a scaffold, binding pigment molecules. The photosynthetic light-harvesting ability therefore depends both on the properties of the pigment moieties and on the protein, which is capable of altering the intrinsic pigment absorption characteristics.

Oxygenic photosynthetic capability is generally based on pigment–protein complexes built around chlorophyll (Chl) *a*. However, it is well known that some cyanobacteria from shaded environments use chlorophylls with substitutions of their porphyrin ring that shift the Q_y absorption band to longer wavelengths and thus allow collecting light beyond the red edge of the Chl *a* absorption. These red-shifted Chls are Chl *d* (major pigment in *Acaryochloris marina*) (Miyashita et al. 1996; Schiller et al. 1997) or Chl *f*, a minor pigment in *Halomicronema hongdechloris* (Chen et al. 2012; Airs et al. 2014; Behrendt et al. 2015; Gan and Bryant 2015). So far, these red-shifted Chls have not been found in eukaryotic algae, which are instead known to rely on the

Electronic supplementary material The online version of this article (https://doi.org/10.1007/s11120-019-00662-5) contains supplementary material, which is available to authorized users.

✉ David Bína
bina@umbr.cas.cz

[1] Faculty of Science, University of South Bohemia, Branišovská 1760, 370 05 České Budějovice, Czech Republic

[2] Biology Centre, The Czech Academy of Sciences, Branišovská 31, 370 05 České Budějovice, Czech Republic

[3] Institute of Microbiology, The Czech Academy of Sciences, Opatovický mlýn, 379 81 Třeboň, Czech Republic

[4] PSI (Photon Systems Instruments), spol. s r.o. Drásov 470, 664 24 Drásov, Czech Republic

pigment–protein and pigment–pigment interactions to tune the absorption spectrum of their light-harvesting system.

Several red-shifted light-harvesting antennas are presently known in eukaryotes. The best understood system is the antenna of plant Photosystem I (PSI), Lhca. Here, the red Chl *a* forms originate from the mixed excitonic and charge transfer (CT) states of Chl dimers (Morosinotto et al. 2003; Romero et al. 2009). Given that the presence of the red Chl *a* forms in Lhca is not associated with shortening of the excited state lifetime, they can be assumed to play the light-harvesting role (Passarini et al. 2010), as suggested before (Trissl 1993).

In contrast to plants, red Chl *a* forms are typically much less prominent in the PSI-associated antennas of algae (Ihalainen et al. 2005; Ikeda et al. 2008; Tichý et al. 2013; Herbstová et al. 2015; Haniewicz et al. 2018). Yet, a number of algal groups are known to employ the red-shifted pigments in the light-harvesting machinery that is connected to PSII or shared between both photosystems (Fujita and Ohki 2004; Wilhelm and Jakob 2006; Kotabová et al. 2014; Herbstová et al. 2015; Wolf et al. 2018). Among green algae, the symbiont of corals *Ostreobium* sp. has been described to possess a significantly red-shifted absorption spectrum (Halldal 1968; Koehne et al. 1999), extending the absorption of its Chl *a/b* system up to 720 nm. Outside of the green lineage, red-shifted antenna systems are known in a number of algal groups with chloroplasts derived by a secondary or tertiary endosymbiotic event—the Stramenopila-Alveolata-Rhizaria (SAR) group of organisms (Janouškovec et al. 2010). *Chromera velia*, also a potential coral symbiont, is a unique alveolate autotroph with a capability to synthesize a red-shifted light harvesting system upon growth in an environment with diminished blue light intensity but sufficient supply of (far-)red light (Bína et al. 2014; Kotabová et al. 2014). The photosynthetic apparatus of *C. velia* is hypothesized to have originated from a stramenopile alga, specifically a relative of eustigmatophytes or chrysophytes (Ševčíková et al. 2015). Another red-shifted light-harvesting complex has been described in a model pennate diatom *Phaeodactylum tricornutum* (Herbstová et al. 2015). Interestingly, the red-shifted light-harvesting antenna systems of *C. velia* and *P. tricornutum* are not directly related and likely have evolved independently. Recently, using far-red illumination as a selection factor, Wolf et al. (2018) isolated a eustigmatophyte alga harboring red-antenna complexes from a freshwater source demonstrating the presence of the far-red adapted light-harvesting outside of marine habitats. In given examples, the presence of red Chl *a* forms manifests itself as strongly red-shifted fluorescence at room temperature even in whole cells in vivo.

In all the above-mentioned eukaryotic algae, the light-harvesting antenna proteins belong to the LHC protein family, which also includes the major antenna proteins of land plants. The LHC protein family shares a basic structural motif of three transmembrane helices Standfuss et al. (2005). The LHC protein family can be generally divided into the group containing Chl *b* (from plants and green algae) and a second group originating in red algae and greatly expanded in the SAR supergroup (Dittami et al. 2010; Hoffman et al. 2011). The function of the SAR-type LHC proteins has been mostly studied in diatoms (Bacillariophyceae), which are a model group of global biogeochemical importance (Bowler et al. 2010). Three major LHC types are found in diatoms: (i) Lhcr-type, usually associated with PSI, with closest homology to the ancestral red algal LHCs; (ii) Lhcf-type, forming the major light-harvesting complexes of diatoms, FCP; (iii) Lhcx-type, a group of LHC proteins associated with photoprotection in analogy to the PsbS protein of plants and including surprisingly also the LhcSR proteins of green algae (Dittami et al. 2010; Hoffman et al. 2011; Zhu and Green 2010; Bonente et al. 2011). The red-shifted LHC proteins described from *C. velia* and *P. tricornutum* form independent sub-clades within the Lhcf clade (Bína et al. 2014; Herbstová et al. 2015).

The red-shifted light-harvesting protein from *C. velia* shares close sequence homology with light-harvesting proteins of eustigmatophyte algae such as *Nannochloropsis* (*N.*) (Bína et al. 2014; Litvín et al. 2016). Motivated by this homology, the light harvesting system of *N. oceanica* was recently analyzed but showed no apparent red-shift upon transfer of cells to red-enhanced light. On the other hand, the purified LHCs of *N. oceanica* (denoted VCP in the eustigmatophytes after Violaxanthin Chlorophyll Protein, Sukenik et al. 2000) had slightly red-shifted absorbance and fluorescence spectra when compared with diatom model systems (Litvín et al. 2016). Very recently, an environmental isolate of a freshwater eustigmatophyte harboring a fully developed red-shifted LHC was described by Wolf et al. (2018) and its antenna system was characterized by biochemical and spectroscopic methods, including the ultrafast time-resolved spectroscopy (Niedzwiedzki et al. 2019). It was also shown that the organism, provisionally denoted FP5, belongs to the same clade within Eustigmatophyceae as *Nannochloropsis, Eustigmatales* (Fawley et al. 2014).

By a fortunate coincidence, we have learned that a recently described eustigmatophyte alga *Trachydiscus minutus* (Přibyl et al. 2012), a distant relative of *Nannochloropsis*, also possesses a fluorescence signature similar to that of the red light-grown *P. tricornutum* or *C. velia*. Like the FP5 strain of Wolf and coworkers, the antenna system of this organism allows purification of reasonably stable preparation of red-shifted LHC which we used to analyze the dynamics of the excitation energy flow (Bína et al. 2019). It was shown that the complex, denoted rVCP, exhibited several properties similar to the (plant) Lhca antenna, such as the multiexponential fluorescence decay, presence of

excitonically coupled chlorophyll molecules and broadened spectral bands suggestive of CT characteristics.

Here we present a detailed account of culture conditions and purification procedures of the rVCP complex and complement the previous time-resolved study by an analysis of its steady-state spectra. Furthermore, we provide a comprehensive characterization of the whole light-harvesting apparatus of *T. minutus*, including the analysis of association of LHC with photosystems. Finally, we attempt to summarize the present knowledge on the red-shifted algal antenna complexes and we discuss possible evolutionary scenarios for the known red LHC complexes.

Materials and methods

Cell growth and conditions

Cells of *Trachydiscus minutus* CCALA 931 were batch-cultured in 5 L Erlenmeyer flasks in a freshwater WC medium (Guillard and Lorenzen 1972) at 20 °C. The cell cultures were stirred and bubbled with filtered air. Illumination was provided by a daylight spectrum metal-halide lamp (OSRAM POWERSTAR HQI-E 70 W/NDL) or by a common halogen light bulb as a red-enhanced light source. In each case the illumination followed a rectangular wave cycle of 15 h light and 9 h dark. Three illumination treatments were used in this study to assess the chromatic acclimation capability of *T. minutus*: (i) daylight spectrum with high intensity of 250 µmol photons m^{-2} s^{-1} (DHL); (ii) low intensity daylight spectrum of 20 µmol photons m^{-2} s^{-1} (DLL); (iii) red-enhanced spectrum with low intensity of 20 µmol photons m^{-2} s^{-1} (RLL). The reader should note that common 'white' incandescent light sources for household use are de facto red/infrared light sources even without further filtering. Broadband illumination spectrum was intentionally used in order to maintain ecologically relevant cultivation conditions using light quality closer to natural environment where monochromatic illumination cannot be assumed (Herbstová et al. 2015).

The fitness of the cells was regularly checked by measuring of the F_v/F_M parameter using an Aquapen device (Photon Systems Instruments, Czech Republic). The F_v/F_M parameters of the studied cultures were 0.64 ± 0.01 (DHL, $n=9$), 0.63 ± 0.01 (DLL, $n=8$) and 0.62 ± 0.02 (RLL, $n=9$). Illumination intensities reported throughout the text were measured by a Hansatech Quantitherm light meter (Hansatech, UK).

Fractionation of pigment–protein complexes

Cells in the late logarithmic phase were collected by centrifugation (7000×*g*, 5 min), washed by distilled water and stored at − 80 °C until further use. For the analysis, cells were washed in 50 mM HEPES buffer (pH 7.5, 2 mM KCl) and resuspended in the same buffer completed with EDTA-free Protease Inhibitor Cocktail (Roche). Subsequently, cells were broken by two passes through an EmulsiFlex-C5 high pressure cell disrupter (Avestin Inc. Canada) at 10,000 psi. The chlorophyll concentration of the disrupted cells was adjusted to 1 mg mL^{-1} and the detergent *n*-dodecyl-β-D-maltoside (β-DM) was added to final concentration of 2% (w/v). The solubilization step was carried out for 15 min with continuous mixing in the dark on ice. After removal of unsolubilized material (30,000×*g*, 20 min, 4 °C), the supernatant was loaded onto a 0.1–1.1 M linear sucrose density gradient prepared in the isolation buffer supplemented with 0.02% β-DM (w/v). Ultracentrifugation was carried out using a SW 40 Ti swing-out rotor (Beckman Coulter, USA) for 17 h at 100,000×*g* at 4 °C. The fractions containing the pigment–protein complexes were collected with a syringe.

Protein composition analyses

Protein complexes pre-purified by the sucrose gradient ultracentrifugation were analyzed by clear native electrophoresis (CN-PAGE) on a 4–14% linear gradient polyacrylamide gel according to Schägger and von Jagow (1991), an upper buffer contained 0.05% sodium deoxycholate and 0.02% β-DM. Samples with 5 µg of total Chl were loaded on the gel. The protein composition of the complexes resolved in the native gel was analyzed by electrophoresis on a denaturing 12% to 20% linear gradient polyacrylamide gel containing 7 M urea (2D-SDS-PAGE) (Komenda et al. 2012). Lanes of interest were excised from the native gel, incubated in 25 mM Tris/HCl (pH 7.5) buffer containing 1% SDS (w/v) and 2% dithiothreitol (w/v) for 30 min and placed on top of the denaturing gel. Proteins separated in the second dimension gel were stained by Coomassie Brilliant Blue.

Optical spectroscopy

Absorbance spectra of cells and bands cut out of the CN-PAGE gels were recorded in a Shimadzu UV-2600 instrument equipped with an integration sphere. Room temperature and low temperature (77 K) fluorescence emission spectra were recorded using Spex Fluorolog-2 spectrofluorometer equipped with double monochromators (Jobin–Yvon, Edison, NJ, USA) with an excitation wavelength of 435 nm, emission slit width of 2 nm and a long pass order sorting filter in the emission path (cut off 460 nm). The room-temperature emission was recorded in a direction perpendicular to the excitation beam, using 1 cm × 1 cm fluorescence cuvettes. The 77 K spectra were recorded using front-face detection on samples immersed in liquid nitrogen in a Dewar vessel using locally made holders. Measured cell cultures

were adjusted to OD_{675} 0.1–0.2. Bands from native gels were cut out on ice and either frozen for 77 K measurements or put into 1 cm × 1 cm fluorescence cuvettes for room temperature absorbance and fluorescence measurements.

Spectrally resolved chlorophyll fluorescence induction curves were excited by a blue LED light source (M470L2, Thorlabs, USA) with illumination intensity in the sample cuvette of 1000 µmol photons m^{-2} s^{-1}. Fluorescence was filtered by a Schott OG-550 glass and detected using a USB4000 spectrometer (OceanOptics, USA) with 1 s detector integration time.

To evaluate differences in cellular fluorescence spectra upon blocking PSII electron transport, DCMU was added to a final concentration of 250 µM. The samples with DCMU were incubated for 5 min in the dark prior to measurement. Fluorescence spectra were measured by the Fluorolog-2 instrument as described above. The intensity of irradiance provided by the measuring beam was below 1 µmol photons m^{-2} s^{-1}. The experiment was carried out in 4 biological replicates.

Spectra of circular dichroism were measured with Jasco J-715 spectropolarimeter. Samples were kept to 4 °C during measurements. The sample of the VCP antenna from *N. oceanica* was purified as described previously (Keşan et al. 2016).

Pigment content analyses

Cellular pigments were extracted on ice in the dark as described previously (Herbstová et al. 2015). Briefly, cells suspended in methanol were sonicated using an ultrasonic homogenizer, the extract was separated by centrifugation and the pellet was subjected to 2 more methanol extractions until it was colorless. All extracts were pooled and dried under vacuum before dissolving in methanol prior to injection into HPLC. Pigments from sucrose gradient zones were extracted analogously, starting with a 50-µL aliquot of sample.

Pigment content was analyzed by HPLC, using the method of Jeffrey et al. (2005), as described previously Litvín et al. (2016). A Zorbax SB-C18 reverse-phase column was used as a stationary phase (4.6 × 150 mm, 5 µm, Agilent, USA). The pigment molar ratios were estimated from the areas under the chromatogram peaks plotted at the wavelengths corresponding to the respective extinction coefficients, corrected by the pigment extinction coefficients. The following molar extinction coefficients (in dm^3 $mmol^{-1}$ cm^{-1}) were used: Chl *a*: 78 at 662 nm; violaxanthin: 153 at 443 nm; vaucheriaxanthin: 154 at 444 nm; β-carotene: 134 at 453 nm (Jeffrey et al. 2005).

Results

Whole cell fluorescence and absorbance spectra

As seen in Fig. 1, fluorescence and absorbance spectra of a culture of *T. minutus* revealed presence of the red-shifted chlorophylls. As a first step of the present study, we analyzed the changes in the contribution of these red Chl *a* forms to the light-harvesting system of *T. minutus* as a response to illumination spectrum and intensity. *T. minutus* cells were grown in three illumination regimes—daylight spectrum in low (20 µE, DLL) and high (250 µE, DHL) intensity and a low intensity (20 µE, RLL) of red-enhanced spectrum (Bína et al. 2014; Herbstová et al. 2015). The room temperature (RT) fluorescence spectra of all three cultures (Fig. 1a) revealed a marked difference to the fluorescence spectrum of a closely related eustigmatophyte species, *N. oceanica*. The maximum of *T. minutus* RT

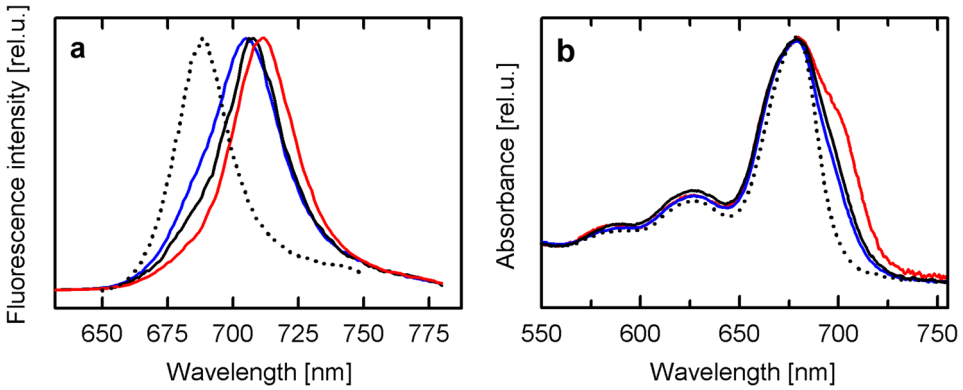

Fig. 1 Room temperature fluorescence (**a**) and absorption (**b**) spectra of the cell cultures of *T. minutus* (blue—cells grown on high intensity daylight spectrum, black—low intensity daylight spectrum, red—red-enhanced spectrum with low intensity) and *N. oceanica* (dotted). Fluorescence spectra were excited at 435 nm. Other experimental details can be found in the materials and methods section. Spectra are representative of at least three biological replicates, the spectra of *N. oceanica* are adapted from Litvín et al. (2016)

fluorescence peaked at 705–711 nm, shifted to the red by 17–23 nm when compared to that of *N. oceanica*. Contrary to the case of *C. velia* and *P. tricornutum*, the maximum of fluorescence in *T. minutus* was above 700 nm even in the cultures grown on high intensity daylight spectrum. The picture was very similar in low temperature (77 K) fluorescence spectra, where all three *T. minutus* cultures emitted above 720 nm (Suppl. Figure 1). The effect of the red-enhanced illumination was also well visible in the absorption spectra, where the RLL cells showed significantly increased absorption around 700 nm (Fig. 1b). The RLL culture absorption was ~40% higher in the region above 690 nm when compared to the DLL and DHL cultures. In contrast to the whole-cells spectra of the red-light enriched eustigmatophyte presented by Wolf et al. (2018; Fig. 1a of the cited work) absorption of our *T. minutus* culture did not extend above 750 nm. However, Wolf and colleagues made no mention of applying any measures to counter the effect of light scattering, such as using an integration sphere. Hence, it can be assumed that their absorbance spectrum of the cell suspension was distorted by scattering, leading to the apparent increase of absorption on the red edge of the Q_y absorption band (Latimer 1959). This explanation is supported by the fact that no antenna complexes absorbing significantly beyond 730 nm were found in subsequent analysis by Wolf et al. (2018).

Kautsky effect and DCMU response in the red fluorescence

In principle, the above-described redshift of fluorescence spectra could be explained by a change in the ratio of photosystems, with photosystem I (PSI) causing an increase of the component above 700 nm. To gain insight into this issue, two spectroscopic experiments were carried out. First, cellular fluorescence spectra were detected during the course of Kautsky fluorescence induction curve. *T. minutus* is known to be capable of a strong NPQ response and the fluorescence yield differs significantly between dark-adapted and light-adapted states (Bína et al. 2017a, b). The spectrum from the initial increase of the fluorescence intensity was then compared with the spectrum after the fluorescence yield reached a steady state (Fig. 2a). The comparison showed that most of the fluorescence above 700 nm followed the induction curve, i.e., there was not a significant constant component expected if PSI had been appreciably contributing to the observed fluorescence spectrum. Second, photosystem II (PSII) inhibitor DCMU was used to increase the yield of PSII to maximum (Fig. 2b). Here again, the comparison of the spectra of dark-adapted cells and cells with added DCMU showed minimal shape differences, demonstrating that most of the observed fluorescence spectrum came from a pigment which was excitonically connected to PSII.

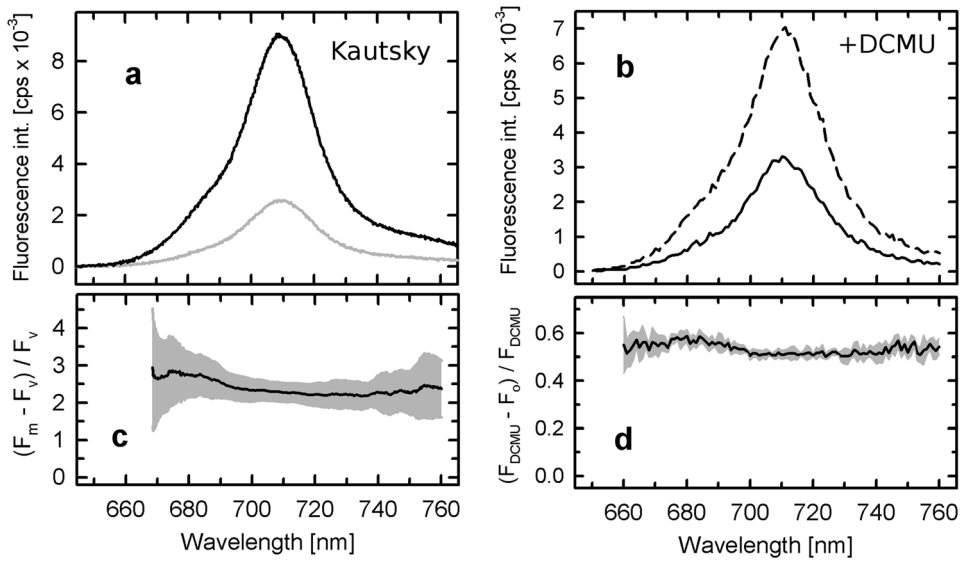

Fig. 2 Variable fluorescence spectra of *T. minutus* RLL cells induced by 1000 µmol photons m^{-2} s^{-1} of blue (470 nm) actinic illumination (**a**) or by DCMU, inhibitor of PSII (**b**). In a, F_m corresponds to maximum fluorescence yield achieved a few seconds after the onset of actinic illumination (black); F_t is a light-adapted fluorescence spectrum (gray). Difference between these two spectra is presented in (**c**), computed as indicated in *y*-axis label. In (**b**), the spectrum of dark-adapted cells F_0 is in black, the spectrum detected after DCMU addition F_{DCMU} is dashed. Difference between the F_0 and F_{DCMU} spectra is shown in (**d**), computed as indicated in *y*-axis label. Computed differences (**c**, **d**) show standard deviation bands in grey ($n=4$). Spectra are representative of four biological replicates

Cellular pigments

The pigment analysis of *T. minutus* cells grown under the three light regimes showed a typical eustigmatophyte pigment composition with violaxanthin, vaucheriaxanthin and Chl *a* as major pigments (Table 1, Suppl. Figure 2). The increased absorption cross section above 690 nm of the RLL cells was therefore caused by the presence of low-energy Chl *a* molecules rather than by a synthesis of a novel Chl species as is the case in some cyanobacteria. In terms of Chl/Car ratios, the RLL culture was more similar to the DHL than to the DLL culture. Violaxanthin was responsible for most of the increase of the total carotenoid content of RLL cells. Interestingly, while all cultures showed similar amounts of total vaucheriaxanthins per Chl *a*, the ratio of vaucheriaxanthin esters was similar in RLL and DLL cells. *T. minutus* cells contained only a minor amount of vaucheriaxanthin-ester when compared with *N. oceanica* (Litvín et al. 2016).

Thylakoid membrane protein composition

Thylakoid membranes of RLL cells were solubilized by β-DM, separated by sucrose gradient ultracentrifugation (Fig. 3a), and further analyzed by CN-PAGE (Fig. 3b) as in Litvín et al. (2016). Selected CN-PAGE lines were then analyzed in a second dimension by SDS-PAGE (Fig. 3c–e). Colored bands identified in CN-PAGE were also analyzed by absorption and fluorescence spectroscopy (Fig. 4, Suppl. Figure 3). The thylakoid proteome analysis of *T. minutus* was based on previous results from three *Nannochloropsis* species (Basso et al. 2014; Litvín et al. 2016; Umetani et al. 2018), which were investigated in the same manner. In contrast to both *Nannochloropsis* species, only small amounts of trimeric or monomeric VCP light harvesting complexes were found in zone Z2 and VCPs were present throughout the sucrose gradient. Zone Z6 of the sucrose gradient predominantly contained PSI of several supercomplex sizes, a situation similar to the related *Nannochloropsis* (Alboresi et al. 2016; Bína et al. 2017a, b). PSII was present mostly in zone Z5 as band B8.

At least four oligomeric VCP complexes differing in size were identified in the CN-PAGE analysis (bands B5, B7, B9 and B10) with zone Z3 containing mostly the two complexes slightly smaller than the PSII monomer (B5 and B7). The largest VCP oligomers were present in zones Z5 and Z6 (B9 and B10) (Fig. 3b), co-purifying with the photosystems. Presence of PSII core just above band B7 helps to estimate its apparent mass about 300 kDa, using the estimate of the PSII monomer mass given by Zouni et al. (2005), which implies ~ 10 LHC subunits (assuming mass of VCP monomer apoprotein of approximately 20 kDa and the pigment complement according to Llansola-Portoles et al. (2017) adding another 10 kDa for a total VCP monomer mass 30 kDa). Here the PSII is assumed to be monomeric based on observation of *N. oceanica* (Bína et al. 2017a, b).

All VCP bands showed increased absorbance on the red edge of the Chl *a* Q_y peak, ranging from just a shoulder in B2 to a distinct peak in the oligomers (Fig. 4, Suppl. Figure 3). The smallest VCP oligomer (B5) showed a relatively high and well-defined red absorption peak at 694 nm. The ratio of the red absorption peak and the main Chl *a* Q_y absorption decreased with increasing size of the antenna complex

Table 1 Pigment composition determined by HPLC analysis of *T. minutus* cells, sucrose gradient zones (labeled Z2–Z6) and fractions from gel filtration analysis of sucrose gradient zone 3 (labeled F1–F4)

	Unknown	Viola	Vauche-ria. + Vauch.-ester	β-car	Vaucheria./ Vauch.-ester	Unknown/Viola (%)	Total carotenoids
Cells DAY LL	1.8 ± 0.1	24.1 ± 1.3	8.9 ± 0.4	4.3 ± 0.7	11.3 ± 0.6	7.5 ± 0.3	39.2 ± 1.4
Cells DAY HL	2.0 ± 0.3	29.0 ± 3.2	9.2 ± 0.7	5.7 ± 0.8	24.2 ± 2.5	6.9 ± 0.3	45.9 ± 4.8
Cells RED LL	2.0 ± 0.3	31.1 ± 5.8	9.6 ± 0.9	7.3 ± 1.6	12.2 ± 3.9	6.5 ± 0.7	50.0 ± 8.0
Z2	1.8 ± 0.1	27.3 ± 2.9	13.3 ± 1.3	1.4 ± 0.6	9.0 ± 2.7	6.5 ± 0.5	43.9 ± 4.2
Z3	1.6 ± 0.6	20.6 ± 2.0	11.6 ± 0.4	1.2 ± 0.7	10.0 ± 2.1	7.8 ± 2.4	34.9 ± 2.0
Z4	1.5 ± 0.6	17.6 ± 4.3	9.2 ± 1.8	3.9 ± 2.7	9.6 ± 1.9	8.0 ± 1.7	32.2 ± 4.0
Z5	0.9 ± 0.4	12.7 ± 2.6	5.5 ± 1.8	8.4 ± 1.2	9.6 ± 2.1	7.0 ± 1.9	27.6 ± 3.6
Z6	0.5 ± 0.2	13.6 ± 1.0	2.5 ± 0.6	8.8 ± 0.4	8.7 ± 1.6	3.8 ± 1.5	25.5 ± 1.2
F1	1.4 ± 0.6	23.9 ± 5.7	13.2 ± 2.5	0.9 ± 0.7	11.2 ± 3.1	5.9 ± 1.1	39.4 ± 8.1
F2	1.4 ± 0.3	19.6 ± 0.5	10.9 ± 1.5	1.7 ± 1.0	9.6 ± 2.5	7.0 ± 1.5	33.6 ± 0.6
F3	0.9 ± 0.3	19.1 ± 0.2	11.7 ± 1.3	1.4 ± 0.8	9.7 ± 2.8	4.7 ± 1.5	33.1 ± 0.3
F4	2.1 ± 0.2	26.4 ± 2.1	13.9 ± 1.8	1.6 ± 0.5	10.4 ± 2.2	7.9 ± 0.3	43.9 ± 2.9

Unless otherwise noted, values are in mol/100 mol Chl *a*. Cell data are averages of at least five biological replicates ± standard deviation. Gradient zone and gel filtration data are averages of three biological replicates. *Viola* Violaxanthin, *Vaucheria* vaucheriaxanthin, *Vauch.-ester* vaucheriaxanthin ester; *β-car* β,β-carotene

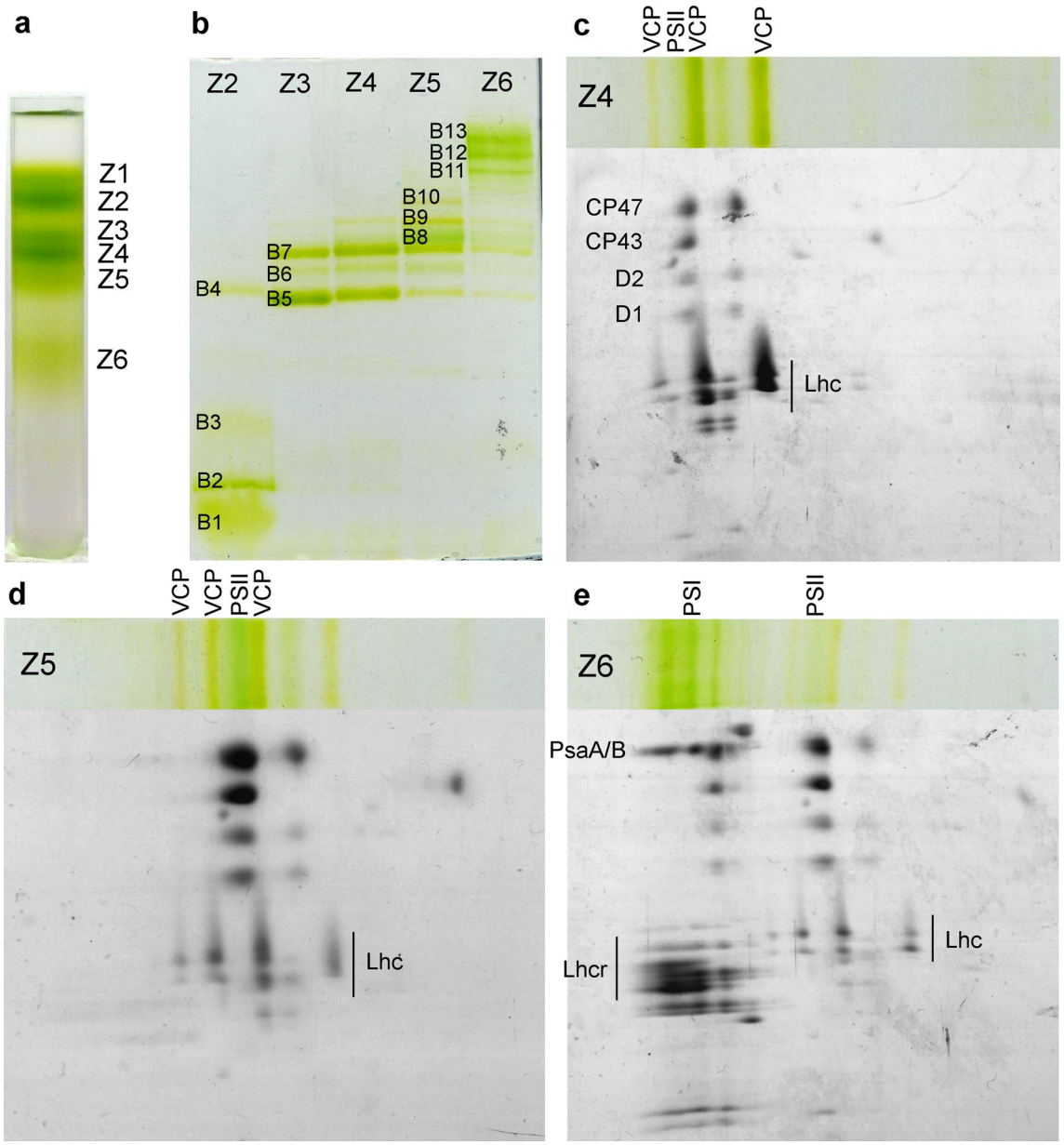

Fig. 3 Analysis of the thylakoid membrane composition of the RLL cells of *T. minutus*. In **a**, sucrose gradient (SG) ultracentrifugation of β-DM solubilized thylakoid membranes is shown. **b** CN-PAGE analysis of SG zones from (**a**). **c–e** 2D-SDS-PAGE analyses of selected lines from CN-PAGE analysis. Respective CN-PAGE lines and selected major proteins are indicated. Protein spots were assigned based on their position in the gels and by comparison with similar analysis of the eustigmatophyte *N. oceanica* (Litvín et al. 2016)

(i.e., from B5 to B10). The red Chl *a* absorption peak was at 700 nm for the largest antenna complexes B9 and B10. All four antenna oligomers in the CN-PAGE gel showed RT fluorescence maxima above 700 nm (Fig. 4a), ranging from 704 nm in B5 to 711 nm in B9 and B10. Contrary to the situation in another eustigmatophyte *N. oceanica* (Litvín et al. 2016), the fluorescence spectra of the larger PSI complexes peaked above 700 nm even at room temperature (bands B12, B13 in Fig. 3a). 77 K fluorescence spectra (Fig. 4b) corroborated the other analyses. At 77 K, the emission maxima of the oligomeric VCP ranged from 710 nm for B5 to 720 nm for B10. PSI fluorescence at 77 K was distinguished by a broader emission band centered at 723–727 nm.

Pigment analysis of the sucrose gradient zones

Pigment composition of the sucrose gradient zones was analyzed to provide information about specific carotenoids used by the thylakoid membrane components. Relative to chlorophyll, total carotenoid content decreased toward

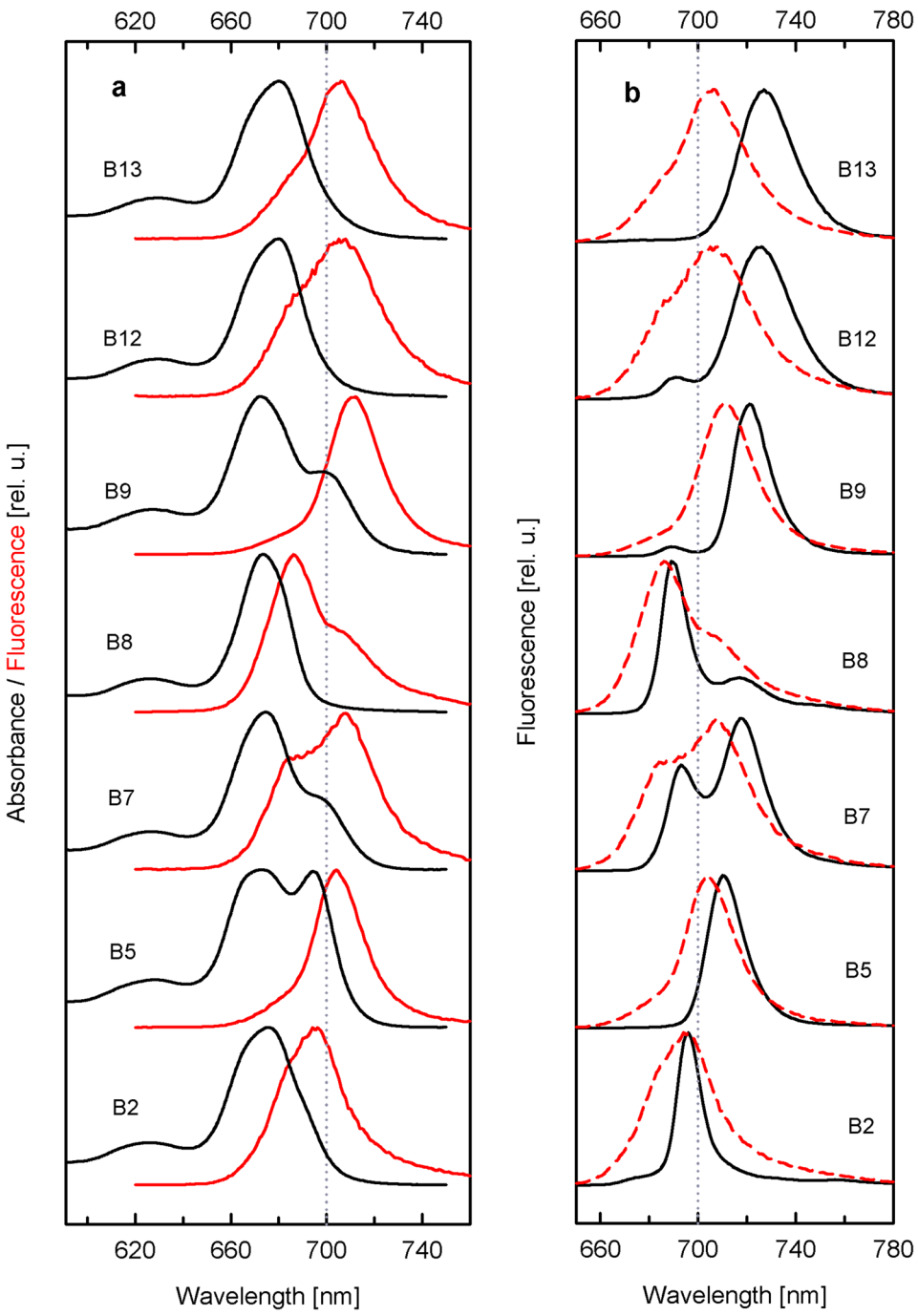

Fig. 4 Spectroscopic analysis of selected CN-PAGE bands presented in Fig. 4b. **a** Room temperature absorbance (black) and fluorescence (red) spectra. **b** Low temperature (77 K) fluorescence spectra (black) and room temperature fluorescence spectra from (**a**) for reader's convenience (dashed red). Bands B2, B5, B7 and B9 are identified in the text as different VCP complexes. Band B8 represents PSII. Bands B12 and B13 represent PSI. See text and Fig. 3 for details of these assignments. For readers' convenience, 700 nm position is indicated by vertical dotted line in both panels

the bottom of the sucrose gradient while the β-car content increased, which was consistent with an increase in photosystem content in the lower parts of the gradient, especially zone Z6 (Table 1). The oligomeric VCP in zone Z3 had Chl *a*/Car ratio of about 2.9, significantly higher than the ratios reported previously for purified VCP trimers of *N. oceanica* (2.2; Keşan et al. 2016) and *N. gaditana* (1.8; Basso et al. 2014). The ratio of violaxanthin to vaucheriaxanthins ranged between 1.8 in Z3 and 2.3 in Z5, and increased to 5.4 in Z6. The xanthophyll ratio of the oligomeric light-harvesting complexes, represented by zone Z3, was close to 2 violaxanthins per 1 vaucheriaxanthin. The light-harvesting antenna of PSI (Z6) contained only small amounts of vaucheriaxanthin yet maintained a high content of violaxanthin.

Purification of the red-shifted VCP complexes

The red-shifted antenna complexes of *T. minutus* survived in significant amounts both sucrose gradient centrifugation and subsequent CN-PAGE analysis and were therefore

apparently much more stable than the corresponding systems of *C. velia* and *P. tricornutum* (Bína et al. 2014; Herbstová et al. 2015). Using sucrose gradient zone Z3 as a starting material, two red-shifted VCP oligomer fractions were purified by the gel filtration chromatography as its major components (Fig. 5a, F2 and F3). Based on their elution volume and absorption spectra (Fig. 5b), these fractions are similar to bands B5 (F3) and B7 (F2) of the CN-PAGE analysis. The pigment content of the two major fractions (F2 and F3) was very similar with ~30 total carotenoids per 100 Chl *a* molecules (Table 1). A SDS-PAGE analysis of the size exclusion chromatography fractions did not show any significant differences in protein composition (Fig. 5c). All four fractions contained mostly low molecular weight proteins of two sizes in a range of 17–20 kDa. These two protein bands were interpreted as at least two distinct light harvesting antenna proteins. The ratio of these protein band intensities did not change among the fractions despite the observed changes in absorption spectra. The dominant fraction F3 was further characterized by optical spectroscopy, see below. Based on the pigment composition and spectroscopic properties, the purified 'red-shifted antenna complex from *T. minutus*' will be referred to simply as rVCP for brevity, in accordance with the recent publication (Bína et al. 2019).

Fluorescence emission spectrum of the rVCP was dominated by a peak with maximum at 700 nm, accompanied by a shoulder around 680 nm (Fig. 5d) at room temperature. Excitation spectrum of the far-red emission (recorded at 715 nm) showed a high efficiency of the energy transfer from carotenoids to the red-shifted Chl *a* forms. This efficiency was highest on the red edge of the carotenoid absorption range, approaching 100%. The more blue-shifted carotenoids at ~480 nm exhibited a lower efficiency (~80%) of the energy transfer, a feature typical of the LHC complexes (e.g., Keşan et al. 2016; Bína et al. 2019). Overall, the carotenoid-to-Chl *a* energy transfer efficiency of our rVCP complex was significantly higher than what was observed in the red-shifted antenna preparation (VCP-B3) of the eustigmatophyte FP5 studied by Niedzwiedzki et al. (2019). Another part of the spectrum that showed a slightly

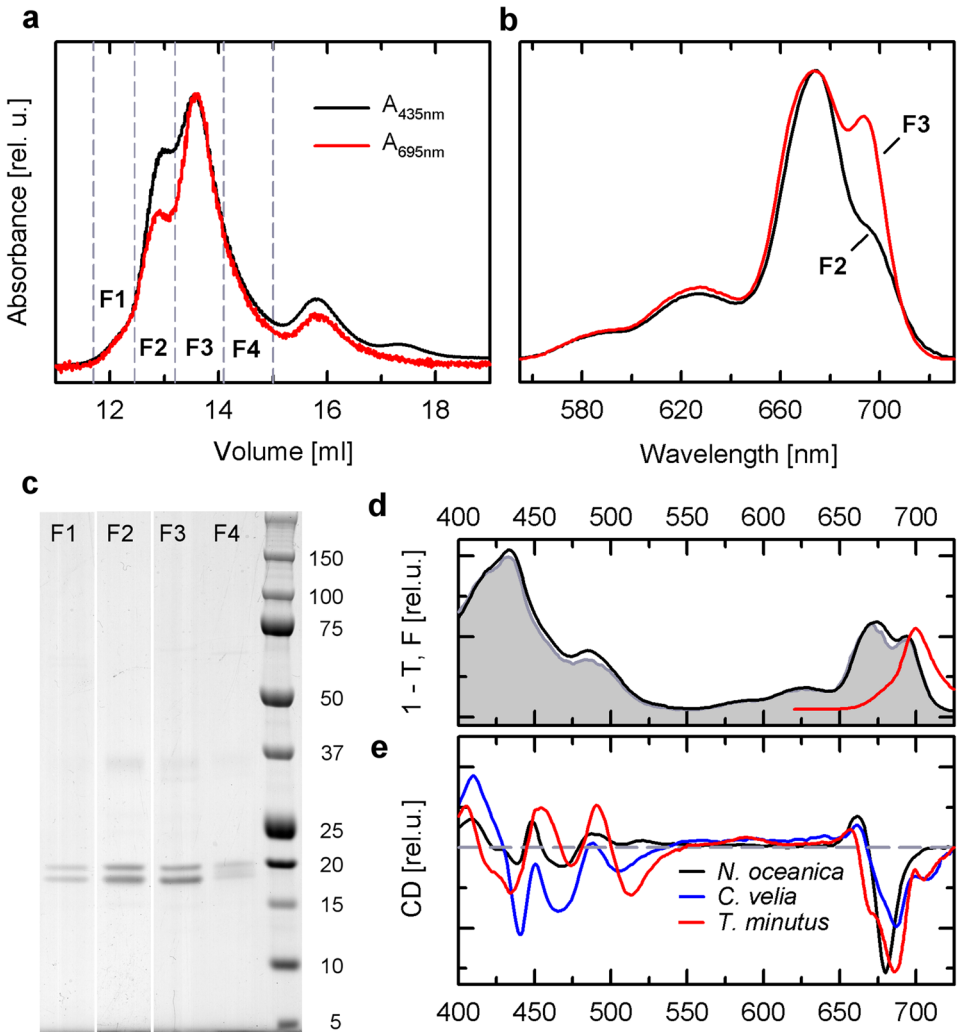

Fig. 5 Analysis of the major rVCPcomplex by gel filtration chromatography of SG zone Z3. Gel filtration chromatograms are presented in (**a**). In **b** are absorption spectra of the two major components purified by the gel filtration chromatography. Protein analysis of the gel filtration fractions by SDS-PAGE is presented in (**c**). Steady-state spectroscopy (at room temperature) of the fraction F3: **d** comparison of 1 − T spectrum (black line) and the excitation spectrum, recorded at 715 nm (grey). Red line shows the emission spectrum. **e** Spectrum of circular dichroism, showing the comparison of the *T. minutus* antenna (red) with the major antenna of another eustigmatophyte, *N. oceanica* (VCP, black, sample prepared as described in Keşan et al. 2016), and the red-shifted antenna complex (red-CLH) from *C. velia* (blue, adapted from Bína et al. 2014)

diminished energy transfer to the red Chl *a*'s lay around 675 nm, most likely indicating a small amount of damaged complexes that lost the red Chl *a* species.

Circular dichroism (CD) is a spectroscopic method that provides insight into the inter-pigment interactions in pigment–protein complexes. It is particularly useful for comparative analysis. In Fig. 5e, the CD spectrum of the rVCP is compared to the VCP antenna of the eustigmatophyte *N. oceanica*, that lacks the pronounced red spectral features, and to the red-shifted antenna complex from *C. velia* (red-CLH). The spectral region 400–500 nm reveals similar structural organization of carotenoids in the three complexes. This is in good agreement with the similar dynamics of the carotenoid-to-Chl *a* energy transfer (Bína et al. 2019) in VCP and rVCP. Moreover, it indicates that oligomerization does not strongly affect the pigment geometry of the LHC core region. It should be stressed that similarities of features in CD spectra do not stem simply from similar pigment composition (see spectra presented in Tichý et al. 2013; Büchel and Garab 1997; Büchel 2003). The feature in the carotenoid spectral region that appears to identify the red-shifted antennas (compared to VCP) is the larger negative signal in the 500–530 nm region, although even in VCP, small but clearly discernible troughs are present in the CD spectrum in this region. The negative signal peaking between 500 and 530 nm is accompanied by a negative band above 700 nm pertinent to the red Chl *a* forms.

In the red region, all three complexes share a positive feature at ~660 nm but the CD spectrum in the region of the Q_y band of Chl *a* is always dominated by a negative band. This appears to be characteristic of the LHC complexes from the algae of the red lineage (Büchel and Garab 1997; Gardian et al. 2014; Jiang et al. 2014; Tichý et al. 2013). In VCP, this peak is narrow with a minimum at 680 nm, in the red antennas it is shifted to ~686 nm and features a shoulder on the blue edge, at ~670 nm, more pronounced in rVCP than in red-CLH. Comparison of the CD spectrum of rVCP to the plant Lhca complexes (Croce et al. 2002; Morosinotto et al. 2003), shows that red forms in both complexes share similar purely negative, i.e., strongly nonconservative CD bands.

Discussion

The analysis presented above showed that the unusual red-shifted fluorescence and absorbance spectra of *T. minutus* cells could be explained by the presence of light harvesting antenna complexes of several oligomeric states with Chl *a* as the only porphyrin pigment. The cellular fluorescence data presented in Figs. 1 and 2 had two key attributes associated with PSII—the Kautsky effect and the response to DCMU. These experiments on living cells of *T. minutus* showed essentially the same pattern as previously found for other algal systems (Bína et al. 2014; Kotabová et al. 2014; Herbstová et al. 2015). In comparison with the diatom *P. tricornutum* (Herbstová et al. 2015), also in *T. minutus* the variable fluorescence signals were slightly (3–4%) enhanced in the area around 680 nm versus the maximum at 710 nm (Fig. 2). This can be interpreted as indicative of a presence of a small fraction of PSII without attached red LHC.

Remarkably, despite the fact that the outer antenna is energetically below the primary donor of PSII reaction center, we have not observed any unusual properties in the PSII core analyzed in CN-PAGE gels (band B8). In fact, the PSII core shown here is effectively identical in composition and in spectroscopy not only to that of other eustigmatophytes but also to diatoms (Nagao et al. 2013). Obtaining larger complexes of stramenopile PSII is apparently difficult (but cf. Nagao et al. 2010; Gardian et al. 2011) and the sensitivity of expected PSII supercomplexes to purification procedures in the majority of analyzed stramenopile thylakoid membranes appears to be one of the more significant differences in the supramolecular arrangement of PSII in comparison with that of the green lineage (de Bianchi et al. 2011; Drop et al. 2014; Bína et al. 2017a, b).

Based on the above-discussed data, the association of rVCP also with PSI could not be ruled out. In fact, the PSI complexes identified in the CN-PAGE gel showed markedly red-shifted (peak emission above 700 nm) fluorescence spectra at room temperature, when compared not only to corresponding complexes from related Eustigmatophytes of the *Nannochloropsis* genus (Basso et al. 2014; Litvín et al. 2016) but also when compared to plant and green algal PSI-LHCI complexes (Ihalainen et al. 2005). The room temperature fluorescence thus identifies *T. minutus* as an alga where multiple pigment–protein complexes exhibit a shift in absorbance to lower energies. That these include the LHC associated with PSI contrasts with the red light-acclimated diatom (Bína et al. 2016) where the PSI-containing membrane patches did not contain any red-FCP.

Regarding the origin of the red-shifted Chl *a* spectral forms, we begin by considering the oligomeric nature of the red antenna complexes. In plant LHC, aggregation is known to induce structural changes that lead to appearance of Chl *a* states characterized by broad emission bands with red-shifted maxima. These states exhibit mixed excitonic and charge transfer (CT) character (Miloslavina et al. 2008; Wahadoszamen et al. 2012, 2016). Although the CT states have been implied as the quenching species in some models of plant photoprotection, this would be difficult to reconcile with the presumed light-harvesting function of the red Chl *a* forms in stramenopiles. Moreover, it should be noted that the CT states do not act as quenchers in the plant PSI antenna (Passarini et al. 2010).

For the purpose of the present analysis, we focus on the 77 K fluorescence of the band B2 that represents the smallest

complex (trimer), and of B5, the simplest of the red-shifted oligomers (Fig. 6). The B2 band peaks at 696 nm and its bandwidth (full width at half maximum, fwhm) is 257 cm^{-1}; the spectrum features a prominent vibrational satellite at 1190 cm^{-1} (759 nm) downhill from the maximum. Thus, the properties of the spectrum of the B2 band correspond to plant LHCII complex at 77 K, as shown, e.g., in Wahadoszamen et al. (2012) and Miloslavina et al. (2008), but shifted by ~ 16 nm (~ 340 cm^{-1}) to lower energies. In comparison, the spectrum of the B5 band peaking at 711 nm is much broader (fwhm = 374 cm^{-1}) and the vibrational band (~ 770 nm) is less pronounced. In Fig. 6 we apply the approach used by the above cited works of Wahadoszamen, Miloslavina and coworkers for analysis of aggregated LHCII to the spectrum of oligomer B5. This consists in decomposing it into an excitonic component and a broad, red-shifted spectral band(s), tentatively ascribed to CT states. Following the cited work, we used the B2 spectrum shifted by ~ 250 cm^{-1} as the excitonic component (in place of LHCII trimer), which was linearly combined with Gaussian bands, representing the probable CT contribution, with following parameters: 712 nm (fwhm 359 cm^{-1}), 725 nm (462 cm^{-1}) and 757 nm (503 cm^{-1}), resulting in an excellent fit of the B5 spectrum. Parameters of the Gaussian bands as well as the amplitude and position of the excitonic band were treated as independent free parameters and optimized together.

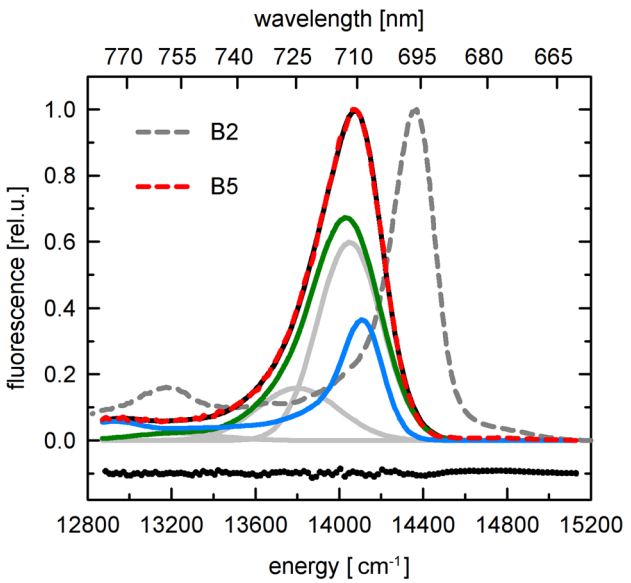

Fig. 6 Comparison of the emission spectra at 77 K of the antenna complexes of bands B2 (trimers, grey dashed line) and B5 (small oligomers, red dashed line). The spectrum of B5 is modeled by a linear combination of an excitonic component (blue) and a broad, red shifted spectral band of CT state (green). The excitonic component of B5 was modeled by using the B2 spectrum, shifted to lower energy (by ~ 250 cm^{-1}). The CT contribution was simulated by linear combination of Gaussian bands with following parameters: 712 nm (fwhm 359 cm^{-1}), 725 nm (462 cm^{-1}) and 757 nm (503 cm^{-1}). Dotted line corresponds to fit residuals

The analysis implies two factors responsible for the development of the red forms in *T. minutus* antenna: (i) pigment–protein interaction determining the properties of the red-shifted excitonic B2-like band; (ii) additional pigment–pigment interactions accompanying the oligomerization probably leading to formation of mixed excitonic-CT states. This very well complements the time resolved spectroscopy data (Bína et al. 2019) that also indicate presence of two red-shifted pools of Chl *a*. Of these, one is in direct contact with light-harvesting carotenoids and the dynamics of the energy transfer is very similar to regular VCP. The excitation is then transferred to more red-shifted forms of Chl *a*, characterized by broadened emission bands with excited state lifetime ~ 2–3 ns, that serve as terminal excitation acceptors in the antenna. Here it is worth noting that another recent study of a red-shifted antenna isolate from Eustigmatophytes (Niedzwiedzki et al. 2019) also revealed multiple, connected Chl *a* pools, manifested in excitation dynamics very similar to rVCP of *T. minutus*.

As seen in Figs. 4 and 5b, the smallest oligomer of *T. minutus* rVCP shows the highest ratio of the 695/685 nm absorbance. Such behavior can be explained by the red Chl state being fully developed in the smallest oligomeric unit (band B5 in Fig. 4b). Adding more LHC units to this system to create a larger complex then does not significantly increase the share of the red Chls in the complex. This can suggest that the larger oligomers (bands B7, B9 and B10) were a biochemical artifact rather than a representation of the native membrane state and the missing red Chls in the larger complexes would be easily explained by nonspecific aggregation of LHCs which would prevent proper pigment positioning. However, both our data and the observations of Wolf et al. (2018) suggest that the larger antenna complexes (B7, B9 and B10 in our case, Figs. 3, 4 and Suppl. Figure 3) are not simply aggregates of the smallest red-shifted Chl *a* complex: a closer inspection of the absorption spectra of the larger complexes reveals that despite the lower amplitude of the red-shifted absorption bands, their edge extends even farther to the red, which is also corroborated by the marked shift toward lower energy of their emission maxima (Fig. 4, Suppl. Figure 3). Hence, some structural change influencing the red Chl *a* species occurs during assembly of the higher antenna oligomers. At present stage one cannot exclude the possibility that oligomers of different size differ also in their polypeptide composition.

The multitude of oligomeric VCP forms found in our analysis is rather striking and in sharp contrast with the situation in related eustigmatophyte species of the genus *Nannochloropsis* (Basso et al. 2014; Litvín et al. 2016) although a limited amount of LHC oligomers was reported from *N. granulata* (Umetani et al. 2018). Both plants (Dekker et al.

1999; Järvi et al. 2011) and stramenopiles (Gardian et al. 2011; Tichý et al. 2013; Gardian et al. 2014) are known to contain larger LHC complexes than trimers. In comparison with an analysis of four diatom species carried out by Nagao et al. (2013), the *T. minutus* VCPs are present in more, and larger, oligomeric forms than in any diatom: some of the LHC oligomers of *T. minutus* are less mobile in CN-PAGE than the PSII core (Nagao et al. 2013).

The present lack of knowledge of the nuclear genome sequence, and thus the LHC, of *T. minutus* hinders comparison to other LHC systems in search for possible molecular determinants of the red shift of Chl *a*. An analysis of the evolutionary path toward this light-harvesting adaptation in different algal groups is also precluded. Available data suggest that the red-light acclimation syndromes of the alveolate *C. velia* and the diatom *P. tricornutum* appear to have developed independently, since they are not accompanied by close homology of the respective antenna proteins (Herbstová et al. 2015). Moreover, the situation in plant PSI antenna proteins (Lhca) suggests that the development of the red-shifted chlorophyll forms can be based on a single amino acid which acts as a ligand to Chl *a* that maintains proper pigment geometry. Replacement of the Chl *a* ligand (Asn) by a different aminoacid (His) was sufficient to eliminate the low-energy spectral bands without disturbing the overall structure and pigment stoichiometry of the pigment–protein complex (Morosinotto et al. 2003).

On the other hand, the data on the algal antennas show that the differences between the red-shifted and "regular" LHC are more far-reaching and, in addition to different degree of oligomerization, always include major differences in pigment binding properties: i) increased chlorophyll to carotenoid ratio was found in diatom and eustigmatophyte red LHCs (this work, Herbstová et al. 2017); ii) in organisms that contain carbonyl-carotenoids (diatoms, *C. velia*), these are depleted in the red LHC, compared to the regular antenna; iii) in diatoms, low Chl *c*/Chl *a* ratio compared to the regular FCP antenna is observed (Herbstová et al. 2017). It should be noted that the lack of Chl *c* is also characteristic of eustigmatophytes, which makes them rather unusual among stramenopiles or algae with secondary plastids of the red origin in general.

A recent phylogenetic analysis (Fawley et al. 2014) revealed that the class Eustigmatophyceae is formed by two major lineages, *Eustigmatales* and *Goniochloridales*, the former represented, e.g., by *Nannochloropsis*, the latter by the 'red-shifted' *Trachydiscus*. However, the red-antenna-harboring freshwater eustigmatophyte recently described by Wolf et al. (2018) belongs to the *Eustigmatales,* hence red antenna is present in both deep-branching clades. This suggests that the trait preceded the divergence. Regarding the relation of "chromerids" and eustigmatophytes, the stramenopile (ochrophyte) origin of the *C. velia* photosynthetic apparatus has been suggested (Ševčíková et al. 2015). The 'eustigmatophyte' pigment composition, namely the absence of chlorophyll *c* and ketocarotenoids of the "chromerid" alga *Vitrella brassicaformis* (Oborník et al. 2012) appears highly significant in this context. Given that the other "chromerid", *C. velia*, appears to have diverged further from the supposed ancestral chloroplast (Ševčíková et al. 2015), its unique ketocarotenoid (iso-fucoxanthin-like) is likely a derived trait of this organism. The other trait of "chromerids" shared with eustigmatophytes is LHC with red-shifted Chl forms (Kotabová et al. 2014 and Suppl. Figure 4), The likely ochrophyte origin of "chromerid" chloroplast (Ševčíková et al. 2015), and the presence of red antenna in both clades within Eustigmatophyceae, supports the parsimony-driven hypothesis of early ochrophyte origin of the adaptation, inherited by eustigmatophytes and "chromerids".

The consequence of this hypothesis is that the absence of the red antenna in genus *Nannochloropsis* is a derived trait. The similarity of *Nannochloropsis* antenna, VCP, and *C. velia* red-CLH in the phylogenetic analysis was noted earlier (Bína et al. 2014) and similarity of antenna systems between the two groups is supported also by the structural similarity of the red-CLH to the VCP of *Nannochloropsis* as revealed by circular dichroism (Fig. 5e). In addition to that, the VCP exhibits a small redshift with respect to the other FCP-like antennas (Litvín et al. 2016), as well as the spectral heterogeneity of the Chl *a* pool (Keşan et al. 2016), not seen in related CLH and XLH antenna systems (Durchan et al. 2012, 2014). For the purpose of discussion, one can entertain the notion that majority of (extant) members of eustigmatophytes are soil and freshwater algae and the move away from the red-shifted system in the predominantly marine *Nannochloropsis* can be explained by a transition toward the planktonic existence in the water column, rich in blue-green, but not red, light (e.g., Herbstová et al. 2017).

Trachydiscus minutus is the second confirmed instance of a freshwater alga harboring a significantly red-shifted light-harvesting system. Unfortunately, limited information exists on the ecology of many known terrestrial algae. The strain used in this work was originally described from cooling pools of a nuclear power plant and only later found also in phytoplankton of fishponds located nearby (Přibyl et al. 2012). Other eustigmatophytes are found also in soils (Andersen 2004), in moderate climates typically shaded by vascular plant foliage. It can be assumed that many species of soil algae would benefit from similar absorption properties and that red-shifted LHCs may be fairly common not only in marine habitats but also on dry land.

The formation of the red-shifted chlorophyll *a*-based LHCs represents a distinct strategy of expanding the range of photosynthetically useful radiation. The main driving force behind this adaptation appears to be the avoidance of (self-)shading in an environment featuring a high

concentration of Chl *a*. As shown using the diatom antenna model (Herbstová et al. 2017), the advantage offered by the increased absorption cross section in the far-red region increases with the density of the algal culture. At the same time, water absorption can be expected to limit the utility of this adaptation to shallow waters. As shown in Sundarabalan and Shanmugam (2015), eutrophic coastal waters are one example of the niche characterized by prominent far-red peak in the spectrum of the downwelling radiation.

As a means of avoiding light limitation in high-chlorophyll, shallow water bodies, the red-shifted Chl *a* forms appear as an attractive direction toward expansion of the light-harvesting abilities of algal cultures intended for mass production of valuable compounds (Blankenship and Chen 2013). The presence of the red-shifted antenna complex in eustigmatophytes, an algal group already showing a promise for industrial application, is thus potentially of great importance. A considerably bolder idea is the introduction of the red-shifted LHC into the plant systems (in addition to the naturally occurring red Chl *a* species of Lhca) to mitigate the shading of the lower leaves, as a part of the "smart canopy" concept as suggested in Ort et al. (2015). The fact that the far-red harvesting LHC evolved independently in different algal lineages and that these systems could be based on the naturally occurring plant pigment, Chl *a*, can be taken as a support of feasibility of such proposal. On the other hand, in all the well-studied far-red LHC systems the full development of the red-shifted Chl *a* forms depends on the formation of supramolecular complexes. Also, it should be noted that in diatoms, the development of the red-shifted LHC was observed as a component of a complex of traits forming a light-limited cell phenotype which included the reorganization of the thylakoid membrane (Bína et al. 2016; Herbstová et al. 2017). Hence it is likely that introduction of such a system into a novel host organism will require not only a modification of the pigment–protein interaction on the level of a single LHC protein chain but must also address the issue of protein–protein interaction and the large-scale organization of the thylakoid membrane, which is different in algal and plant chloroplast. The inherent complexity of such manipulation notwithstanding, the red-shifted LHC in our opinion deserve attention in the context of the quest toward improved photosynthetic yield for food and biofuel production.

Acknowledgements This research was supported by the Czech Science Foundation under the Grant Numbers 19-28323X (Radek Litvín, David Bína) and GA15-22000S (Martin Trtílek), by institutional support RVO:60077344, Project LO1416 Algatech plus of the programme NPU I (Marek Pazderník, Eva Kotabová, Ondřej Prášil), and European Regional Development Fund (No. CZ.02.1.01/0.0/0.0/15_003/0000441, Zdenko Gardian). Skilled technical assistance of Ivana Hunalová and František Matoušek is gratefully acknowledged.

Compliance with ethical standards

Conflict of interest The authors declare that they have no conflict of interest.

References

Airs R, Temperton B, Sambles C, Farnham G, Skill S, Llewellyn C (2014) Chlorophyll f and chlorophyll d are produced in the cyanobacterium *Chlorogloeopsis fritschii* when cultured under natural light and near-infrared radiation. FEBS Lett 588:3770–3777

Alboresi A, Le Quiniou C, Yadav SKN, Scholz M, Meneghesso A, Gerotto C, Simionato D, Hippler M, Boekema EJ, Croce R, Morosinotto T (2016) Conservation of core complex subunits shaped the structure and function of photosystem I in the secondary endosymbiont alga *Nannochloropsis gaditana*. New Phytol 213:714–726

Andersen RA (2004) Biology and systematics of heterokont and haptophyte algae. Am J Bot 91:1508–1522

Basso S, Simionato D, Gerotto C, Segalla A, Giacometti GM, Morosinotto T (2014) Characterization of the photosynthetic apparatus of the Eustigmatophycean *Nannochloropsis gaditana*: evidence of convergent evolution in the supramolecular organization of photosystem I. Biochim Biophys Acta 1837:306–314

Behrendt L, Brejnrod A, Schliep M, Sørensen SJ, Larkum AW, Kühl M (2015) Chlorophyll f-driven photosynthesis in a cavernous cyanobacterium. ISME J 9:2108–2111

Bína D, Gardian Z, Herbstová M, Kotabová E, Koník P, Litvín R, Prášil O, Tichý J, Vácha F (2014) Novel type of red-shifted chlorophyll a antenna complex from *Chromera velia* II. Biochemistry and spectroscopy. Biochim Biophys Acta 1837:802–810

Bína D, Herbstová M, Gardian Z, Vácha F, Litvín R (2016) Novel structural aspect of the diatom thylakoid membrane: lateral segregation of photosystem I under red-enhanced illumination. Sci Rep 6:25583

Bína D, Bouda K, Litvín R (2017a) A two-component nonphotochemical fluorescence quenching in eustigmatophyte algae. Photosynth Res 131:65–77

Bína D, Gardian Z, Herbstová M, Litvín R (2017b) Modular antenna of photosystem I in secondary plastids of red algal origin: a *Nannochloropsis oceanica* case study. Photosynth Res 131:255–266

Bína D, Durchan M, Kuznetsova V, Vácha F, Litvín R (2019) Energy transfer dynamics in a red-shifted violaxanthin-chlorophyll a light-harvesting complex. Biochim Biophys Acta 1860:111–120

Blankenship RE, Chen M (2013) Spectral expansion and antenna reduction can enhance photosynthesis for energy production. Curr Opin Chem Biol 17:457–461

Bonente G, Ballottari M, Truong TB, Morosinotto T, Ahn TK, Fleming GR, Niyogi KK, Bassi R (2011) Analysis of LhcSR3, a protein essential for feedback de-excitation in the green alga *Chlamydomonas reinhardtii*. PLoS Biol 9:e1000577

Bowler C, Vardi A, Allen AE (2010) Oceanographic and biogeochemical insights from diatom genomes. Annu Rev Mar Sci 2:333–365

Büchel C (2003) Fucoxanthin–chlorophyll proteins in diatoms: 18 and 19 kDa subunits assemble into different oligomeric states. Biochemistry 42:13027–13034

Büchel C, Garab G (1997) Organization of the pigment molecules in the chlorophyll a/c light-harvesting complex of *Pleurochloris meiringensis* (xanthophyceae). Characterization with circular dichroism and absorbance spectroscopy. J Photochem Photobiol, B 37:118–124

Chen M, Li Y, Birch D, Willows RD (2012) A cyanobacterium that contains chlorophyll f—a red-absorbing photopigment. FEBS Lett 586:3249–3254

Croce R, Morosinotto T, Castelletti S, Breton J, Bassi R (2002) The Lhca antenna complexes of higher plants photosystem I. Biochim Biophys Acta 1556:29–48

de Bianchi S, Betterle N, Kouřil R, Cazzaniga S, Boekema E, Bassi R, Dall'Osto L (2011) *Arabidopsis* mutants deleted in the light-harvesting protein Lhcb4 have a disrupted photosystem II macrostructure and are defective in photoprotection. Plant Cell 23:2659–2679

Dekker JP, van Roon H, Boekema EJ (1999) Heptameric association of light-harvesting complex II trimers in partially solubilized photosystem II membranes. FEBS Lett 449:211–214

Dittami SM, Michel G, Collén J, Boyen C, Tonon T (2010) Chlorophyll-binding proteins revisited—a multigenic family of light-harvesting and stress proteins from a brown algal perspective. BMC Evol Biol 10:365

Drop B, Webber-Birungi M, Yadav SKN, Filipowicz-Szymanska A, Fusetti F, Boekema EJ, Croce R (2014) Light-harvesting complex II (LHCII) and its supramolecular organization in *Chlamydomonas reinhardtii*. Biochim Biophys Acta 1837:63–72

Durchan M, Tichý J, Litvín R, Šlouf V, Gardian Z, Hříbek P, Vácha F, Polívka T (2012) Role of carotenoids in light-harvesting processes in an antenna protein from the chromophyte *Xanthonema debile*. J Phys Chem B 116:8880–8889

Durchan M, Keşan G, Šlouf V, Fuciman M, Staleva H, Tichý J, Litvín R, Bína D, Vácha F, Polívka T (2014) Highly efficient energy transfer from a carbonyl carotenoid to chlorophyll a in the main light harvesting complex of *Chromera velia*. Biochim Biophys Acta 1837:1748–1755

Fawley K, Eliáš M, Fawley M (2014) The diversity and phylogeny of the commercially important algal class Eustigmatophyceae, including the new clade Goniochloridales. J Appl Phycol 26:1773–1782

Fujita Y, Ohki K (2004) On the 710 nm fluorescence emitted by the diatom *Phaeodactylum tricornutum* at room temperature. Plant Cell Physiol 45:392–397

Gan F, Bryant DA (2015) Adaptive and acclimative responses of cyanobacteria to far-red light. Environ Microbiol 17:3450–3465

Gardian Z, Tichý J, Vácha F (2011) Structure of PSI, PSII and antennae complexes from yellow-green alga *Xanthonema debile*. Photosynth Res 108:25–32

Gardian Z, Litvín R, Bína D, Vácha F (2014) Supramolecular organization of fucoxanthin–chlorophyll proteins in centric and pennate diatoms. Photosynth Res 121:79–86

Guillard R, Lorenzen C (1972) Yellow-green algae with chlorophyllide c. J Phycol 8:10–14

Halldal P (1968) Photosynthetic capacities and photosynthetic action spectra of endozoic algae of the massive coral *Favia*. The Biological Bulletin 134:411–424

Haniewicz P, Abram M, Nosek L, Kirkpatrick J, El-Mohsnawy E, Olmos JDJ, Kouřil R, Kargul JM (2018) Molecular mechanisms of photoadaptation of photosystem I supercomplex from an evolutionary cyanobacterial/algal intermediate. Plant Physiol 176:1433–1451

Herbstová M, Bína D, Koník P, Gardian Z, Vácha F, Litvín R (2015) Molecular basis of chromatic adaptation in pennate diatom *Phaeodactylum tricornutum*. Biochim Biophys Acta 1847:534–543

Herbstová M, Bína D, Kaňa R, Vácha F, Litvín R (2017) Red-light phenotype in a marine diatom involves a specialized oligomeric red-shifted antenna and altered cell morphology. Sci Rep 7:11976

Hoffman GE, Sanchez Puerta MV, Delwiche CF (2011) Evolution of light-harvesting complex proteins from Chl c-containing algae. BMC Evol Biol 11:101

Ihalainen JA, van Stokkum IHM, Gibasiewicz K, Germano M, van Grondelle R, Dekker JP (2005) Kinetics of excitation trapping in intact Photosystem I of *Chlamydomonas reinhardtii* and *Arabidopsis thaliana*. Biochim Biophys Acta 1706:267–275

Ikeda Y, Komura M, Watanabe M, Minami C, Koike H, Itoh S, Kashino Y, Satoh K (2008) Photosystem I complexes associated with fucoxanthin–chlorophyll-binding proteins from a marine centric diatom. Biochim Biophys Acta 1777:351–361

Janouškovec J, Horák A, Oborník M, Lukeš J, Keeling PJ (2010) A common red algal origin of the apicomplexan, dinoflagellate, and heterokont plastids. Proc Natl Acad Sci USA 107:10949–10954

Järvi S, Suorsa M, Paakkarinen V, Aro E-M (2011) Optimized native gel systems for separation of thylakoid protein complexes: novel super- and mega-complexes. Biochem J 439:207–214

Jeffrey S, Mantoura R, Wright S (2005) Phytoplankton pigments in oceanography: guidelines to modern methods, 2nd edn. UNESCO Publishing, Paris

Jiang J, Zhang H, Orf GS, Lu Y, Xu W, Harrington LB, Liu H, Lo CS, Blankenship RE (2014) Evidence of functional trimeric chlorophyll a/c2-peridinin proteins in the dinoflagellate *Symbiodinium*. Biochim Biophys Acta 1837:1904–1912

Keşan G, Litvín R, Bína D, Durchan M, Šlouf V, Polívka T (2016) Efficient light-harvesting using non-carbonyl carotenoids: energy transfer dynamics in the VCP complex from *Nannochloropsis oceanica*. Biochim Biophys Acta 1857:370–379

Koehne B, Elli G, Jennings RC, Wilhelm C, Trissl HW (1999) Spectroscopic and molecular characterization of a long wavelength absorbing antenna of *Ostreobium* sp. Biochim Biophys Acta 1412:94–107

Komenda J, Knoppová J, Kopečná J, Sobotka R, Halada P, Yu J, Nickelsen J, Boehm M, Nixon PJ (2012) The Psb27 assembly factor binds to the CP43 complex of photosystem II in the cyanobacterium *Synechocystis* sp. PCC 6803. Plant Physiol 158:476–486

Kotabová E, Jarešová J, Kaňa R, Sobotka R, Bína D, Prášil O (2014) Novel type of red-shifted chlorophyll a antenna complex from *Chromera velia*. I. Physiological relevance and functional connection to Photosystems. Biochim Biophys Acta 1837:734–743

Latimer P (1959) Influence of selective light scattering on measurements of absorption spectra of *Chlorella*. Plant Physiol 34:193

Litvín R, Bína D, Herbstová M, Gardian Z (2016) Architecture of the light-harvesting apparatus of the eustigmatophyte alga *Nannochloropsis oceanica*. Photosynth Res 130:137–150

Llansola-Portoles MJ, Litvín R, Ilioaia C, Pascal AA, Bína D, Robert B (2017) Pigment structure in the violaxanthin–chlorophyll-a-binding protein VCP. Photosynth Res 134:51–58

Miloslavina Y, Wehner A, Lambrev PH, Wientjes E, Reus M, Garab G, Croce R, Holzwarth AR (2008) Far-red fluorescence: a direct spectroscopic marker for LHCII oligomer formation in non-photochemical quenching. FEBS Lett 582:3625–3631

Miyashita H, Ikemoto H, Kurano N, Adachi K, Chihara M, Miyachi S (1996) Chlorophyll *d* as a major pigment. Nature 383:402

Morosinotto T, Breton J, Bassi R, Croce R (2003) The nature of a chlorophyll ligand in Lhca proteins determines the far red fluorescence emission typical of photosystem I. J Biol Chem 278:49223–49229

Nagao R, Tomo T, Noguchi E, Nakajima S, Suzuki T, Okumura A, Kashino Y, Mimuro M, Ikeuchi M, Enami I (2010) Purification and characterization of a stable oxygen-evolving Photosystem II complex from a marine centric diatom, *Chaetoceros gracilis*. Biochim Biophys Acta 1797:160–166

Nagao R, Takahashi S, Suzuki T, Dohmae N, Nakazato K, Tomo T (2013) Comparison of oligomeric states and polypeptide compositions of fucoxanthin chlorophyll a/c-binding protein complexes among various diatom species. Photosynth Res 117:281–288

Niedzwiedzki DM, Wolf BM, Blanenship RE (2019) Excitation energy transfer in the far-red absorbing violaxanthin/vaucheriaxanthin

chlorophyll a complex from the eustigmatophyte alga FP5. Photosynth Res. https://doi.org/10.1007/s11120-019-00615-y
Oborník M, Modrý D, Lukeš M, Cernotíková-Stříbrná E, Cihlář J, Tesařová M, Kotabová E, Vancová M, Prášil O, Lukeš J (2012) Morphology, ultrastructure and life cycle of *Vitrella brassicaformis* n. sp, n. gen, a novel chromerid from the Great Barrier Reef. Protist 163:306–323
Ort DR, Merchant SS, Alric J et al (2015) Redesigning photosynthesis to sustainably meet global food and bioenergy demand. Proc Natl Acad Sci USA 112:8529–8536
Passarini F, Wientjes E, van Amerongen H, Croce R (2010) Photosystem I light-harvesting complex Lhca4 adopts multiple conformations: red forms and excited-state quenching are mutually exclusive. Biochim Biophys Acta 1797:501–508
Přibyl P, Eliáš M, Cepák V, Lukavský J, Kaštánek P (2012) Zoosporogenesis, morphology, ultrastructure, pigment composition, and phylogenetic position of *Trachydiscus minutus* (Eustigmatophyceae, Heterokontophyta). J Phycol 48:231–242
Romero E, Mozzo M, van Stokkum IHM, Dekker JP, van Grondelle R, Croce R (2009) The origin of the low-energy form of photosystem I light-harvesting complex Lhca4: mixing of the lowest exciton with a charge-transfer state. Biophys J 96:L35–L37
Schägger H, von Jagow G (1991) Blue native electrophoresis for isolation of membrane protein complexes in enzymatically active form. Anal Biochem 199:223–231
Schiller H, Senger H, Miyashita H, Miyachi S, Dau H (1997) Light-harvesting in *Acaryochloris marina*—spectroscopic characterization of a chlorophyll d-dominated photosynthetic antenna system. FEBS Lett 410:433–436
Ševčíková T, Horák A, Klimeš V, Zbránková V, Demir-Hilton E, Sudek S, Jenkins J, Schmutz J, Přibyl P, Fousek J, Vlček Č, Lang BF, Oborník M, Worden AZ, Eliáš M (2015) Updating algal evolutionary relationships through plastid genome sequencing: did alveolate plastids emerge through endosymbiosis of an ochrophyte? Sci Rep 5:10134
Standfuss J, Terwisscha van Scheltinga AC, Lamborghini M, Kühlbrandt W (2005) Mechanisms of photoprotection and nonphotochemical quenching in pea light-harvesting complex at 2.5 A resolution. EMBO J 24:919–928
Sukenik A, Livne A, Apt KE, Grossman AR (2000) Characterisation of a gene encoding the light-harvesting violaxanthin–chlorophyll protein of *Nannochloropsis* sp. (Eustigmatophyceae). J Phycol 36:563–570
Sundarabalan B, Shanmugam P (2015) Modelling of underwater light fields in turbid and eutrophic waters: application and validation with experimental data. Ocean Sci 11:33–52
Tichý J, Gardian Z, Bína D, Koník P, Litvín R, Herbstová M, Pain A, Vácha F (2013) Light harvesting complexes of *Chromera velia*, photosynthetic relative of apicomplexan parasites. Biochim Biophys Acta 1827:723–729
Trissl H-W (1993) Long-wavelength absorbing antenna pigments and heterogeneous absorption bands concentrate excitons and increase absorption cross section. Photosynth Res 35:247–263
Umetani I, Kunugi M, Yokono M, Takabayashi A, Tanaka A (2018) Evidence of the supercomplex organization of photosystem II and light-harvesting complexes in *Nannochloropsis granulata*. Photosynth Res 136:49–61
Wahadoszamen Md, Berera R, Ara AM, Romero E, van Grondelle R (2012) Identification of two emitting sites in the dissipative state of the major light harvesting antenna. Phys Chem Chem Phys 14:759–766
Wahadoszamen Md, Belgio E, Rahman MA, Ara AM, Ruban AV, van Grondelle R (2016) Identification and characterization of multiple emissive species in aggregated minor antenna complexes. Biochim Biophys Acta 1857:1917–1924
Wilhelm C, Jakob T (2006) Uphill energy transfer from long-wavelength absorbing chlorophylls to PS II in *Ostreobium* sp. is functional in carbon assimilation. Photosynth Res 87:323–329
Wolf BM, Niedzwiedzki DM, Magdaong NCM, Roth R, Goodenough U, Blankenship RE (2018) Characterization of a newly isolated freshwater Eustigmatophyte alga capable of utilizing far-red light as its sole light source. Photosynth Res 135:177–189
Zhu S-H, Green BR (2010) Photoprotection in the diatom *Thalassiosira pseudonana*: role of LI818-like proteins in response to high light stress. Biochim Biophys Acta 1797:1449–1457
Zouni A, Kern J, Frank J, Hellweg T, Behlke J, Saenger W, Irrgang K-D (2005) Size determination of cyanobacterial and higher plant Photosystem II by gel permeation chromatography, light scattering, and ultracentrifugation. Biochemistry 44:4572–4581

Publisher's Note Springer Nature remains neutral with regard to jurisdictional claims in published maps and institutional affiliations.